J|A|C|S
ARTICLES
Published on Web 08/16/2006

Conformational Flexibility of a Microcrystalline Globular Protein: Order Parameters by Solid-State NMR Spectroscopy

Justin L. Lorieau and Ann E. McDermott*

Contribution from the Department of Chemistry, Columbia University, Havemeyer Hall, 3000 Broadway, New York, New York 10027

Received April 14, 2006; E-mail: aem5@columbia.edu

Abstract: The majority of protein structures are determined in the crystalline state, yet few methods exist for the characterization of dynamics for crystalline biomolecules. Solid-state NMR can be used to probe detailed dynamic information in crystalline biomolecules. Recent advances in high-resolution solid-state NMR have enabled the site-specific assignment of ^{13}C and ^{15}N nuclei in proteins. With the use of multidimensional separated-local-field experiments, we report the backbone and side chain conformational dynamics of ubiquitin, a globular microcrystalline protein. The measurements of molecular conformational order parameters are based on heteronuclear dipolar couplings, and they are correlated to assigned chemical shifts, to obtain a global perspective on the sub-microsecond dynamics in microcrystalline ubiquitin. A total of 38 Cα, 35 Cβ and multiple side chain unique order parameters are collected, and they reveal the high mobility of ubiquitin in the microcrystalline state. In general the side chains show elevated motion in comparison with the backbone sites. The data are compared to solution NMR order parameter measurements on ubiquitin. The SSNMR measurements are sensitive to motions on a broader time scale (low microsecond and faster) than solution NMR measurements (low nanosecond and faster), and the SSNMR order parameters are generally lower than the corresponding solution values. Unlike solution NMR relaxation-based order parameters, order parameters for $^{13}C^1H_2$ spin systems are readily measured from the powder line shape data. These results illustrate the potential for detailed, extensive, and site-specific dynamic studies of biopolymers by solid-state NMR.

Introduction

Solid-state NMR studies have significant capabilities for characterizing dynamics on a wide range of time scales,[1] for example through the measurement of anisotropic dipolar,[2−4] quadrupolar[5−7] and chemical shielding[8] interactions, which contain detailed dynamic information on the molecule.[2,9,10] In contrast with other biophysical tools such as solution NMR and X-ray crystallography, solid-state NMR (SSNMR) can be used to study amorphous and insoluble systems and probe detailed information related to anisotropic interactions and therefore to motional mechanism.[11]

Recent advances in multidimensional solid-state NMR[12−15] have enabled the site-specific assignment of chemical shifts for individual ^{13}C and ^{15}N nuclei.[16−19] In turn, progress in site-specific assignment has stimulated the biophysical characterization of multiple sites in a protein molecule. Many studies have focused on the characterization of a few sites in a protein molecule.[2,3,9] However, an extensive site-specific characterization with multiple-spin system types remains to be studied by SSNMR. Here we show the measurement of $^{13}C^1H_x$ order parameters throughout the ubiquitin protein in a precipitated state, including site-specifically assigned measurements in 38 Cα, 35 Cβ, and multiple side-chain sites. These measurements are made using the dipolar tensor, a quantitative probe that is sensitive to motion on a microseconds and faster time scale and, therefore, significantly slower time scales than the corresponding solution generalized order parameter[20,21] as measured by relaxation studies.

(1) Palmer, A. G.; Williams, J.; McDermott, A. *J. Phys. Chem.* **1996**, *100*, 13293−13310.
(2) Huster, D.; Xiao, L. S.; Hong, M. *Biochemistry* **2001**, *40*, 7662−7674.
(3) Hong, M.; Yao, X. L.; Jakes, K.; Huster, D. *J. Phys. Chem. B* **2002**, *106*, 7355−7364.
(4) Franks, W. T.; Zhou, D. H.; Wylie, B. J.; Money, B. G.; Graesser, D. T.; Frericks, H. L.; Sahota, G.; Rienstra, C. M. *J. Am. Chem. Soc.* **2005**, *127*, 12291−12305.
(5) Usha, M. G.; Wittebort, R. J. *J. Mol. Biol.* **1989**, *208*, 669−678.
(6) Mack, J. W.; Usha, M. G.; Long, J.; Griffin, R. G.; Wittebort, R. J. *Biopolymers* **2000**, *53*, 9−18.
(7) Usha, M. G.; Speyer, J.; Wittebort, R. J. *Chem. Phys.* **1991**, *158*, 487−500.
(8) Cole, H. B. R.; Torchia, D. A. *Chem. Phys.* **1991**, *158*, 271−281.
(9) Yao, X. L.; Conticello, V. P.; Hong, M. *Magn. Reson. Chem.* **2004**, *42*, 267−275.
(10) Williams, J.; McDermott, A. *Biochemistry* **1995**, *34*, 8309−8319.
(11) McDermott, A. E. *Curr. Opin. Struct. Biol.* **2004**, *14*, 554−561.
(12) Andrew, E. R.; Bradbury, A.; Eades, R. G. *Nature* **1958**, *182*, 1656.
(13) Hester, R. K.; Ackerman, J. L.; Cross, V. R.; Waugh, J. S. *Phys. Rev. Lett.* **1975**, *34*, 993−995.
(14) van Rossum, B.-J.; de Groot, C. P.; Ladizhansky, V.; Vega, S.; de Groot, H. J. M. *J. Am. Chem. Soc.* **2000**, *122*, 3465−3472.
(15) Takegoshi, K.; Nakamura, S.; Terao, T. *J. Chem. Phys.* **2003**, *118*, 2325−2341.
(16) McDermott, A.; Polenova, T.; Bockmann, A.; Zilm, K. W.; Paulsen, E. K.; Martin, R. W.; Montelione, G. T. *J. Biomol. NMR* **2000**, *16*, 209−219.
(17) Igumenova, T. I.; McDermott, A. E.; Zilm, K. W.; Martin, R. W.; Paulson, E. K.; Wand, A. J. *J. Am. Chem. Soc.* **2004**, *126*, 6720−6727.
(18) Igumenova, T.; Wand, A.; McDermott, A. *J. Am. Chem. Soc.* **2004**, *126*, 5323−5331.
(19) Pauli, J.; Baldus, M.; van Rossum, B.; de Groot, H.; Oschkinat, H. *ChemBioChem* **2001**, *2*, 272−281.

Solid-state NMR dipolar order parameters are measured using the anisotropic interaction; since the sample does not reorient isotropically in a solution, the molecular frame remains fixed in the solid-state, and thus a direct measurement of the tensor is possible. In eq 1, motional narrowing of an axially symmetric anisotropic coupling is characterized by an order parameter ($\langle S \rangle$), which is averaged during molecular motion over a time scale spanning from the characteristic time scale of the tensorial interaction itself, up to arbitrarily fast time scales. Therefore, order parameters measure the amplitude of motions in the so-called "fast-limit," i.e., the rate constant exceeds all frequencies of the Hamiltonian,[22] which is typically tens of microseconds[23] for heteronuclear dipolar couplings ($^{13}C^1H_x$) in organic solids. The order parameter describing motion with the simplifying assumption of cylindrical symmetry is listed in eq 1. In contrast, eq 2 describes the generalized order parameter measured in NMR relaxation experiments.

$$\langle S \rangle = \frac{1}{2}\langle 3\cos^2(\theta) - 1 \rangle \quad (1)$$

$$S^2 = \sum_m \langle Y_{2m}(\theta',\phi') \rangle^2 \quad (2)$$

In practice, order parameters can be measured in SSNMR experiments by comparing the experimental tensor breadth to that expected for an analogous tensor probed for a rigid molecule. The fast-limit motional amplitude that is characterized by the order parameter ($\langle S \rangle$) ranges from 1 (rigid motion) to 0 (isotropic motion). Equations relating the order parameter to the angular extent of motion have been derived for specific simple motion models such as the N-site hop or cone-diffusion.[1,24] For example, the diffusion in a cone equation is:

$$\langle S \rangle = \frac{\langle \cos(\theta) \rangle + \langle \cos^2(\theta) \rangle}{2}$$

$$\langle \eta \rangle = 0 \quad (3)$$

Typically, solid-state NMR measurements of tensors, including studies of order parameters, have been conducted on samples with a few site-specifically isotopically enriched sites,[2,3,8] or on an unresolved spectrum of many sites.[5−7,25,26] These experiments include the dynamics study of ^{2}H-methyl-labeled retinal in bacteriorhodopsin,[27] the study of the aggregate of deuterium-exchanged amide sites in lysozyme,[6] and the study of water molecule dynamics in the microcrystalline SH3 domain of α-spectrin.[28] Recently, new developments in high-resolution SSNMR have enabled the site-specific assignment of ^{13}C and ^{15}N chemical shifts for uniformly ^{13}C/^{15}N-labeled BPTI,[16] ubiquitin,[17,18] the α-spectrin SH3 domain,[19] and other biomolecular systems. High-resolution solid-state NMR is achieved by combining multidimensional pulse-sequences with magic-angle spinning (MAS).[12] MAS consists of high-frequency rotation of the sample at ∼54.7° to suppress the anisotropic contribution of the magnetic interaction Hamiltonian. The result is a high-resolution isotropic spectrum with chemical shift resonances from individual sites in the molecule. Recoupling sequences can be used to selectively reintroduce the anisotropic components of the Hamiltonian and correlate them to the high-resolution chemical shift. Accordingly, the detailed information content of the magnetic interaction anisotropy can be probed at individual sites, using high-resolution MAS recoupling pulse-sequences. Recently, site-specific dynamic measurements were achieved by solid-state NMR. Huster et al.[2] measured backbone and side-chain $^{13}C^1H$ order parameters in a few sites with the Colicin Ia channel, revealing backbone order parameters as low as 0.9. Franks et al.[4] measured backbone $^{13}C^1H$ and $^{15}N^1H$ order parameters of GB1 with a DIPSHIFT T-MREV (transverse Mansfield−Rhim−Elleman−Vaughan) experiment, measuring backbone order parameters as low as 0.75.

In this study, we used multidimensional recoupling sequences to probe the order parameters of microcrystalline uniformly ^{13}C/^{15}N-enriched ubiquitin, a 76-residue protein with mixed α/β secondary structure, using the heteronuclear (^{13}C−^{1}H) dipolar coupling tensor as our entrée to probe motional averaging. We were able to probe 137 dipolar order parameters with 38 unique Cα backbone sites and 35 Cβ, 13 Cγ, 4 Cδ, and 1 Cε unique side-chains sites. The measurements are distributed throughout the molecule, giving a global picture of the conformational dynamics of ubiquitin in the solid state. We utilized a simple three-dimensional (3D) experiment in which the $^{13}C^1H_x$ heteronuclear dipolar order parameters were probed using a Lee−Goldburg cross-polarization recoupling period (t_1), and the ^{13}C isotropic chemical shifts were resolved in two dimensions (t_2, and the t_3) using the dipolar assisted rotational resonance (DARR) experiment; the 3D experiment is therefore referred to as a LGCP-DARR experiment.[13−15]

Methods and Materials

Measurements were conducted on a Bruker 750 MHz wide-bore NMR spectrometer with a standard-bore probe in ^{1}H/^{13}C/^{15}N configuration. A ^{1}H Lee−Goldburg field of 73.8 kHz and TPPM decoupling[34] field of 68.0 kHz were used. A DARR field of 14 kHz (equal to the spinning speed) was applied for a period of 50 ms. The LGCP-DARR experiment correlates the $^{13}C^1H_x$ dipolar spectrum in t_1 to the ^{13}C chemical shift in t_2, and the ^{13}C chemical shift acquisition dimension t_3 further disperses the sites (see Supporting Information for a pulse sequence diagram). Data were collected with a sweep width of 36.900 kHz (44 points, zero-filled to 256 points), 14.286 kHz (214 points, zero-filled to 512 points) and 71.429 kHz (1750 points, zero-filled to 4096 points) in t_1, t_2, and t_3, respectively. Each 3D experiment consisted of 16 scans, and the experimental time of each experiment was 5.2 days. Exponential line broadening was used in t_1 (1.5 kHz) and t_3 (50 Hz), and sine-square bell was used in t_2.

(20) Wand, A. J.; Urbauer, J. L.; Mcevoy, R. P.; Bieber, R. J. *Biochemistry* **1996**, *35*, 6116−6125.
(21) Schneider, D. M.; Dellwo, M. J.; Wand, A. J. *Biochemistry* **1992**, *31*, 3645−3652.
(22) Long, J. R.; Sun, B. Q.; Bowen, A.; Griffin, R. G. *J. Am. Chem. Soc.* **1994**, *116*, 11950−11956.
(23) Torchia, D. A. *J. Magn. Reson.* **1985**, *64*, 135−141.
(24) Wittebort, R. J.; Olejniczak, E. T.; Griffin, R. G. *J. Chem. Phys.* **1987**, *86* (10), 5411−5420.
(25) Sparks, S. W.; Cole, H. B. R.; Torchia, D. A.; Young, P. E. *Chem. Scr.* **1989**, *29A*, 31−38.
(26) Lewis, B. A.; Harbison, G. S.; Herzfeld, J.; Griffin, R. G. *Biochemistry* **1985**, *24*, 4671−4679.
(27) Copie, V.; McDermott, A. E.; Beshah, K.; Williams, J. C.; Spijkerassink, M.; Gebhard, R.; Lugtenburg, J.; Herzfeld, J.; Griffin, R. G. *Biochemistry* **1994**, *33*, 3280−3286.
(28) Chevelkov, V.; Faelber, K.; Diehl, A.; Heinemann, U.; Oschkinat, H.; Reif, B. *J. Biomol. NMR* **2005**, *31*, 295−310.
(29) Henry, E. R.; Szabo, A. *J. Chem. Phys.* **1985**, *82*, 4753−4761.
(30) Case, D. A. *J. Biomol. NMR* **1999**, *15*, 95−102.
(31) Koetzle, T. F.; Golic, L.; Lehmann, M. S.; Verbist, J. J.; Hamilton, W. C. *J. Chem. Phys.* **1974**, *60*, 4690−4696.
(32) Langan, P.; Mason, S. A.; Myles, D.; Schoenborn, B. P. *Acta Crystallogr., Sect. B: Struct. Sci.* **2002**, *58*, 728−733.
(33) Lorieau, J. L.; McDermott, A. E. *Magn. Reson. Chem.* **2006**, *44*, 334−347.
(34) Bennett, A. E.; Rienstra, C. M.; Auger, M.; Lakshmi, K. V.; Griffin, R. G. *J. Chem. Phys.* **1995**, *103*, 6951−6958.

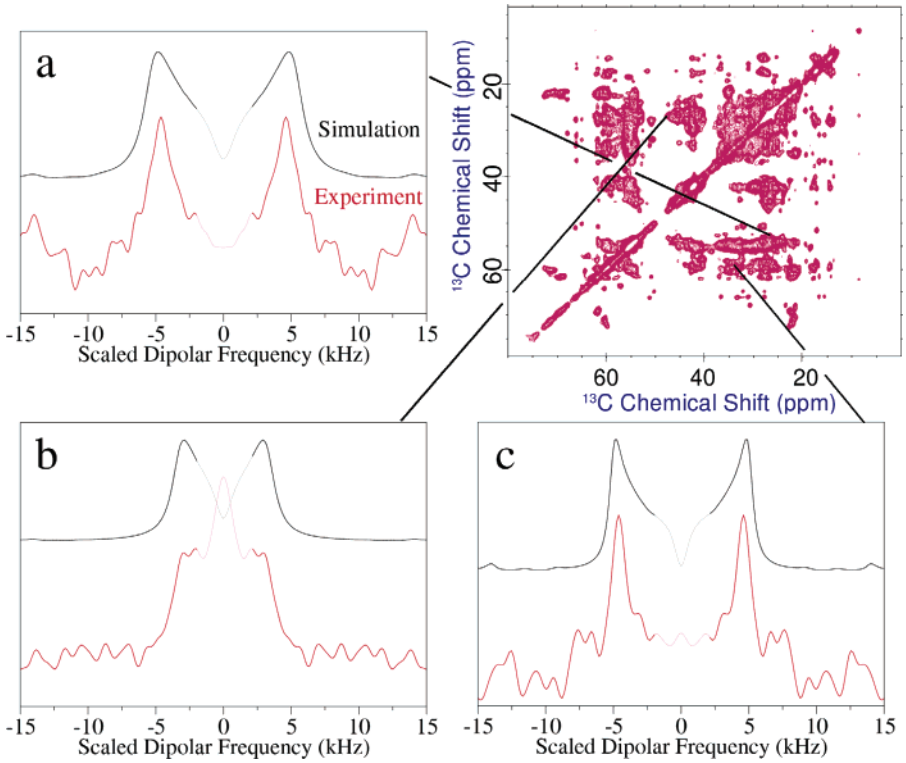

Figure 1. Site-specific $^{13}C^{1}H$ dipolar spectra from microcrystalline uniformly labeled $^{13}C/^{15}N$ ubiquitin. Dipolar spectra are shown for (a) Leu-15 $^{13}C^{1}H\alpha/\langle S\rangle = 0.83 \pm 0.05$, (b) Leu-15 $^{13}C^{1}H\gamma/\langle S\rangle = 0.52 \pm 0.06$ and (c) Lys-27 $^{13}C^{1}H\alpha/\langle S\rangle = 0.79 \pm 0.03$. The dipolar splitting is scaled by the Lee−Goldburg irradiation, and the experimental scaling constant is 0.577. The 2D $^{13}C-^{13}C$ plot is generated by summing all of the planes in the t_1 time domain. The vertical axis is the t_2/indirect ^{13}C chemical dimension, and the horizontal axis is the t_3/direct ^{13}C chemical shift dimension. The zero frequency component is the result of the CP build-up. This range is not included in fitting the dipolar spectra, and it is shaded out in the dipolar spectra.

The microcrystalline U-^{13}C,^{15}N-ubiquitin sample was prepared as previously described,[17,18] and it was sealed with rubber spacers in a 4-mm Bruker rotor to prevent evaporative loss of water. The sample volume was 27 μL, and the estimated B_1 homogeneity of the probe was about 90−95% on both ^{1}H and ^{13}C channels. The MAS spinning speed was 14.00 kHz, and the sample temperature was 17 °C after calibration of the heating to due MAS spinning—the heating due to RF irradiation is unknown.

Automated data analysis was conducted with a customized C++ program using the gamma library.[35] The program uses a list of cross-peak assignments from peak maxima in t_2 and t_3,[17,18] and it extracts the dipolar spectra within ±2 or ±3 points (±0.3 or ±0.3 ppm) in t_2 and t_3, respectively. The cross-peaks were assigned from previously published ^{13}C chemical shift tables for microcrystalline U-^{13}C,^{15}N-ubiquitin.[17,18] The acquired spectral resolution and apodization in t_2/t_3 is comparable to this range, and decomposing t_1 of each cross-peak shows the variability and overlap in dipolar spectra. Another program was developed to easily find overlapping and new cross-peaks within ±0.5 ppm from the list of known ^{13}C resonances and sequential contacts within ±1 residue. With the output of this program, cross-peaks with multiple assignments were rejected from the order parameter analysis due to the ambiguity of assignment.

The peaks and corresponding experimental dipolar spectra are automatically sorted according to spin-system type ($^{13}C^{1}H$ or $^{13}C^{1}H_2$). Each dipolar spectrum is then fit against a series of simulations with variable order parameters ($\langle S\rangle$: 0.22−1.07; $\langle \eta\rangle = 0$) and exponential line broadening (1.5−6.5 kHz). The measured dipolar coupling constant is scaled in the LG experiment by a constant that depends on the magic angle, the ^{1}H on-resonance field and the ^{1}H offset from the carrier frequency, and the cross-polarization match condition. The theoretical scaling constant is $3^{-1/2}$,[14] and the experimentally calibrated scaling constant is 0.577. The experimental scaling factor is calculated from the experimental fields from the protein sample; calibration of the scaling factor from small molecules is inaccurate because the B_1 and ω_{off} fields are different on a protein sample. The LGCP simulations used the experimentally calibrated ^{1}H fields and the $n = -1$ CP condition. The error in the absolute value of the order parameter is estimated on the basis of the expression for the scaling factor[14] and standard first-order propagation of error; assuming a 2 kHz error in the ^{1}H Lee−Goldburg offset frequency, a 2 kHz error in the on-resonance ^{1}H frequency, and the 0.1 kHz inaccuracy in the calculated static dipolar coupling constant the result is 0.05. Relative errors in order parameters predominantly arise from chemical shift differences—see the section on bias in the order measurements. The source of variability in the exponential line broadening is unclear, but the dominant contribution is likely from $T_{1\rho}$ and B_1 inhomogeneity.

The χ^2 and single-parameter 95% confidence interval are characterized for each cross-peak reported. The line broadening and dipolar coupling are not covariant.[36] The zero-frequency component of the dipolar spectra is not included in the fit. Dipolar spectra were fit from ±12 to ±3 kHz. The zero-frequency component is not meaningful because of the DC offset artifacts and data processing routines. Moreover, it is present in model compounds known to be static, and therefore no dynamic information was extracted from the zero frequency component. With the line broadening applied, this means that a range of ±3 kHz cannot be interpreted. On the basis of the χ^2 minimum and the signal-to-noise, the best-fit dipolar spectrum for each cross-peak is selected and inspected manually. The χ^2 minima range from 2.4 to 61; on the basis of a study of LGCP on small crystalline molecules, high χ^2 minima might be attributed to (among other things) low signal-to-noise and poor B_1 homogeneity.[33] LGCP simulations show that poor B_1 homogeneity will broaden and distort the line shape for $^{13}C^{1}H$ and $^{13}C^{1}H_2$ spin systems.[33]

(35) Smith, S. A.; Levante, T. O.; Meier, B. H.; Ernst, R. R. *J. Magn. Reson. Series a* **1994**, *106*, 75−105.

(36) Lorieau, J. L. *Protein Dynamics*; Columbia University: New York, 2005.

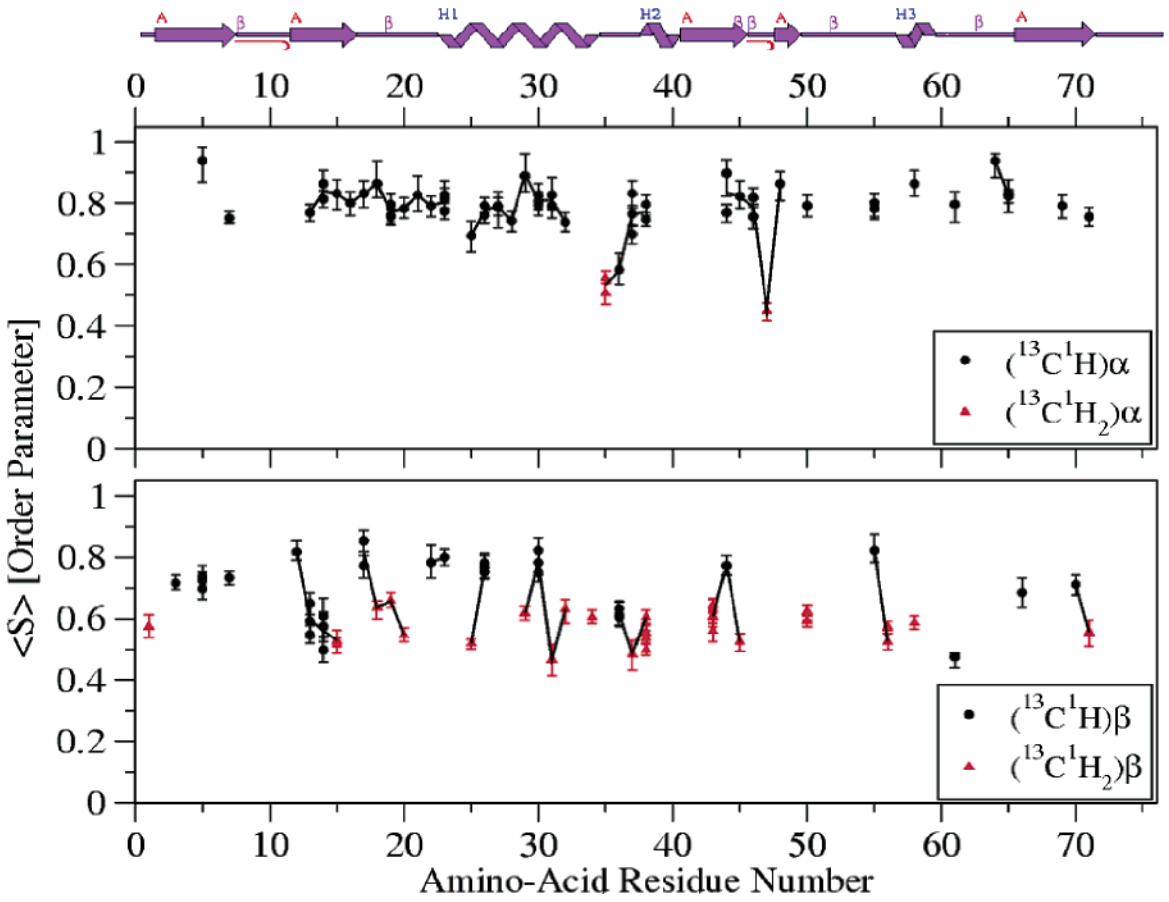

Figure 2. Solid-state NMR dipolar order parameters for ($^{13}C^1H_x$)α and ($^{13}C^1H_x$)β spin systems in microcrystalline uniformly labeled ubiquitin. Order parameters are calculated from the motionally narrowed dipolar coupling, using eq 1. Black lines represent regions with sequential order parameters. Wire plot generated with PDBsum.[53,54]

The order parameter is measured from the reduced dipolar coupling constant with eq 1, where the calculated static limit dipolar coupling constant is 22.5 ± 0.1 kHz—based on the Cα−Hα bond length for L-alanine[29−31] and glycine,[32] 1.102 ± 0.002 Å. The dipolar coupling is compensated for ultrafast vibrational averaging,[29,30] using the same procedure as is done in solution NMR by extending the crystallographic $^{13}C^1H$ bond radius by 1%.[29] ^1H nuclei that are not directly bonded to the ^{13}C nucleus were not included in the simulation, and it was found that their effect on the accuracy of the order parameter measurement is negligible from small molecule studies.[33]

Results and Discussion

A few representative dipolar spectra and a 2D projection spectrum of the $^{13}C-^{13}C$ chemical shift dimensions from the 3D are shown in Figure 1. Since the t_2 dimension of multiple cross-peaks can share the same dipolar coupling of a site, the dataset contains multiple measurements for many individual sites. The majority of redundant order parameters were within the 95% confidence interval of each other, and only a few sites had multiple order parameter measurements with 95% confidence intervals that did not overlap.

Although the 2D DARR collapse spectrum appears symmetric about the diagonal, the mirrored cross-peaks above and below the diagonal report on different dipoles. The dipolar recoupling dimension in t_1 is correlated to the ^{13}C chemical shift in t_2. Although the diagonal is higher in intensity than the cross-peaks, it has the poor site resolution of a ^{13}C one-dimensional spectrum, and therefore, it could not be used for site-specific assignments.

The microcrystalline ubiquitin backbone ($^{13}C^1H_x$)α and ($^{13}C^1H_x$)β order parameters are plotted in Figure 2. Sites are missing from the dataset because (1) not all ^{13}C chemical shifts have been identified for microcrystalline ubiquitin[17,18] (typically due to peak overlap), (2) the dipolar spectrum of a cross-peak was ambiguous (multiple dipolar splittings and/or inconsistency throughout the peak), or (3) the peak was absent due to intermediate exchange. In the case of intermediate exchange, reorientation of the dipolar tensor during the microsecond to submillisecond time scale of the pulse sequence will significantly diminish the efficiency of cross polarization as well as homo- and heteronuclear decoupling. For example, the highly mobile loop regions that span residues 5−12 and 53−55 are missing from this dataset. A previous study in our group demonstrated[33] that LGCP could be used to measure accurate dipolar couplings from $^{13}C^1H$, $^{13}C^1H_2$, and $^{13}C^1H_3$ spin systems in the presence of weak ^1H and one-bond ^{13}C homonuclear couplings, using simple spin systems. In contrast to measurements of order parameters from solution NMR relaxation experiments, the measurement of order parameters for $^{13}C^1H_2$ is straightforward by solid-state NMR from the powder line shape.

The ($^{13}C^1H$)α order parameters for microcrystalline ubiquitin range from 0.58 to 0.94, and the glycine ($^{13}C^1H_2$)α order parameters range from 0.45 to 0.56. For reference, solid-state NMR order parameters of 0.98−1.03 have been measured in alanine at room temperature and glycine at −45 °C for ($^{13}C^1H$)α and ($^{13}C^1H_2$)α systems,[36] respectively, as well as in protein systems [data not shown] by LGCP. Therefore, we conclude that the backbone of ubiquitin in the microcrystalline state is highly dynamic on the microsecond to picosecond time scale.

Depending on the motional model assumed, e.g. motion in a cone, this range of $\langle S \rangle$ values corresponds to an angular excursion of 16°−47° for ($^{13}C^1H$)α and 48°−55° for ($^{13}C^1H_2$)α. The most dynamic sites include Gly-35 and Ile-36, which are at the C-terminus of α-helix 1, and Gly-47, which participates in a β-hairpin. The residues adjacent to Gly-47 have higher order parameters, and their backbones participate in shorter hydrogen-bonding interactions than Gly-47. Few ($^{13}C^1H_x$)α have order parameters near 1.0; the most static sites are Val-5 and Glu-64 with ($^{13}C^1H_x$)α parameters of 0.94 ± 0.07 and 0.94 ± 0.05, respectively. These two residues participate in β-sheets.

The ($^{13}C^1H$)β and ($^{13}C^1H_2$)β order parameters span a larger range than the backbone ($^{13}C^1H$)α (not including the glycine sites). The ($^{13}C^1H$)β and ($^{13}C^1H_2$)β order parameters range between 0.48 and 0.85 and 0.47−0.66, respectively. If the diffusion in a cone[1] is used to model the dynamic motion, the corresponding cone diffusion angles are 29°−53° for ($^{13}C^1H$)β and 41°−54° for ($^{13}C^1H_2$)β. Despite crystal contact interactions and a constrained volume, the protein molecules remain highly dynamic. Moreover, ($^{13}C^1H$)β groups are noticeably less dynamic than ($^{13}C^1H_2$)β groups. Isoleucine, valine, and threonine residues have branched substituents at the Cβ position, and the more highly substituted ($^{13}C^1H$)β sites are more rigid. The ($^{13}C^1H$)β and ($^{13}C^1H_2$)β order parameters show that the side chains are highly mobile on the picosecond to microsecond time scale for microcrystalline ubiquitin.

Protein side chains are generally shown to be more mobile than the corresponding backbone sites in this study. For example, the backbone and side-chain order parameters for leucine, lysine, and proline are shown in Figure 3. In all three cases, the order parameters on the side chain are lower than those of the backbone, indicating greater mobility in the side chain.

The ($^{13}C^1H_2$)β sites of leucine residues are more mobile than those of the backbone, and the ($^{13}C^1H_2$)γ sites have order parameters similar to those of the corresponding ($^{13}C^1H_2$)β site. The leucine ($^{13}C^1H_2$)γ order parameter is inherently less mobile due to the bulk of two methyl groups. The lysine 29 order parameters decrease as you advance down the aliphatic side chain, analogous to phospholipid studies,[37] reaching a limiting value of 0.45−0.52 at the ($^{13}C^1H_2$)γ site.

Comparison to Solution NMR. Comparisons between liquid-phase generalized order parameters derived from the Lipari−Szabo analysis of relaxation data, liquid-phase residual dipolar coupling based (RDC-based) order parameters and solid-state NMR order parameters are shown in Figure 4. In addition to the differences in sample environments for solution and solid states, the principles allowing for order parameter measurement are very different. The solid-state order parameter is sensitive to motions that are on the submicrosecond time scale, while in contrast, the Lipari−Szabo solution NMR generalized order parameter is sensitive to motions on the picosecond to nanosecond time scale. The RDCs are averaged on the millisecond to microsecond time scale, and therefore the order parameters derived from these experiments are expected to be more comparable to those from solid-state NMR. In Figure 4, a 1:1 line is drawn in red to show that most ($^{13}C^1H$)α order parameters are lower in the solid-state than solution NMR, which indicates that motions faster than the microsecond but slower than nanosecond time scale are significant in ubiquitin. Moreover,

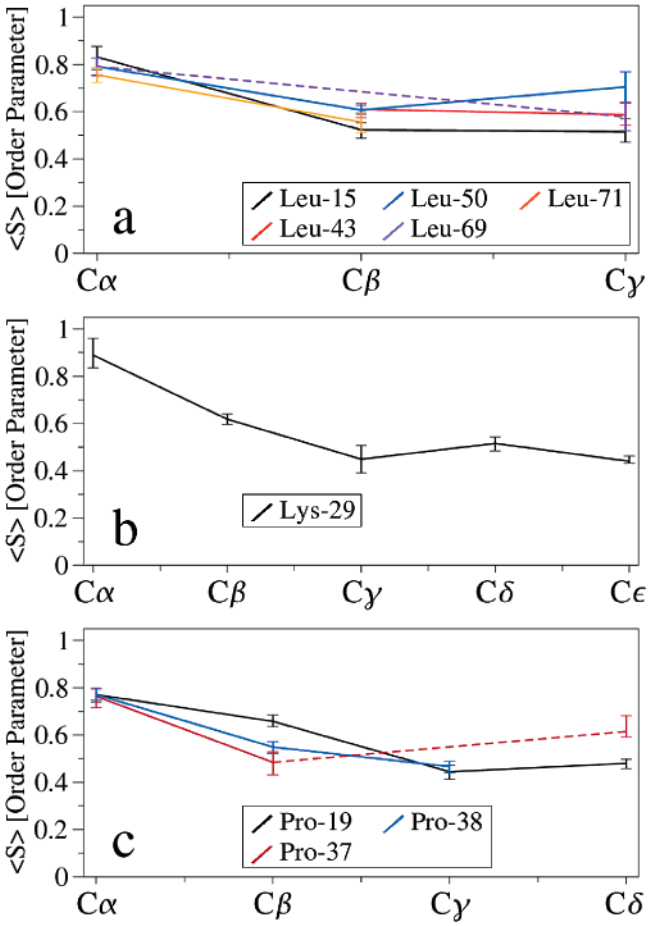

Figure 3. Side-chain order parameter dynamics for (a) leucine, (b) lysine, and (c) proline residues of microcrystalline ubiquitin. Average order parameters and χ^2 errors are reported for sites with multiple measurements. (a) ($^{13}C^1H_2$)β and ($^{13}C^1H$)γ sites are more dynamic than the backbone. Similarities in side-chain dynamics exist between residues of the same amino acid type. The dashed line indicates that the ($^{13}C^1H_2$)β site is not assigned for residue 69. (b) Side-chain order parameters for lysine 29. The order parameters decrease along the side chain, and the ($^{13}C^1H_2$)γ, ($^{13}C^1H_2$)δ, and ($^{13}C^1H_2$)ϵ sites have similar order parameters. (c) Side-chain order parameters for proline show that the backbone is more static than the side chains. For Pro-19 and Pro-38, the ($^{13}C^1H_2$)β is more static than other side-chain sites, and for Pro-37, the ($^{13}C^1H_2$)δ is more static.

there is no strong correlation between the Lipari−Szabo solution and solid-state parameters, indicating that the sample environments may be different and that motion in the submicrosecond regime may not directly correlate with the amount of motion in the subnanosecond regime. On the other hand, the RDC-based order parameters have a weak positive correlation to the SSNMR order parameters.

The solid-state NMR order parameter is generally smaller than the Lipari−Szabo solution NMR generalized order parameter, and this inequality is easily rationalized on the basis of the difference in time scale. For example, Ile-36 is significantly below the 1:1 at (0.99,0.58), indicating significant submicrosecond motions that are not detected on the relaxation solution NMR time scale. It is known that Lys-11 forms a salt bridge with Glu-34[38,39] in the 1UBQ crystal structure,[40] and this salt-

(37) Seelig, J.; Seelig, A. *Q. Rev. Biophys.* **1980**, *13*, 19−61.

(38) Makhatadze, G. I.; Loladze, V. V.; Ermolenko, D. N.; Chen, X. F.; Thomas, S. T. *J. Mol. Biol.* **2003**, *327*, 1135−1148.
(39) Zech, S. G.; Wand, A. J.; McDermott, A. E. *J. Am. Chem. Soc.* **2005**, *127*, 8618−8626.
(40) Vijay-Kumar, S.; Bugg, C. E.; Cook, W. J. *J. Mol. Biol.* **1987**, *194*, 531−544.

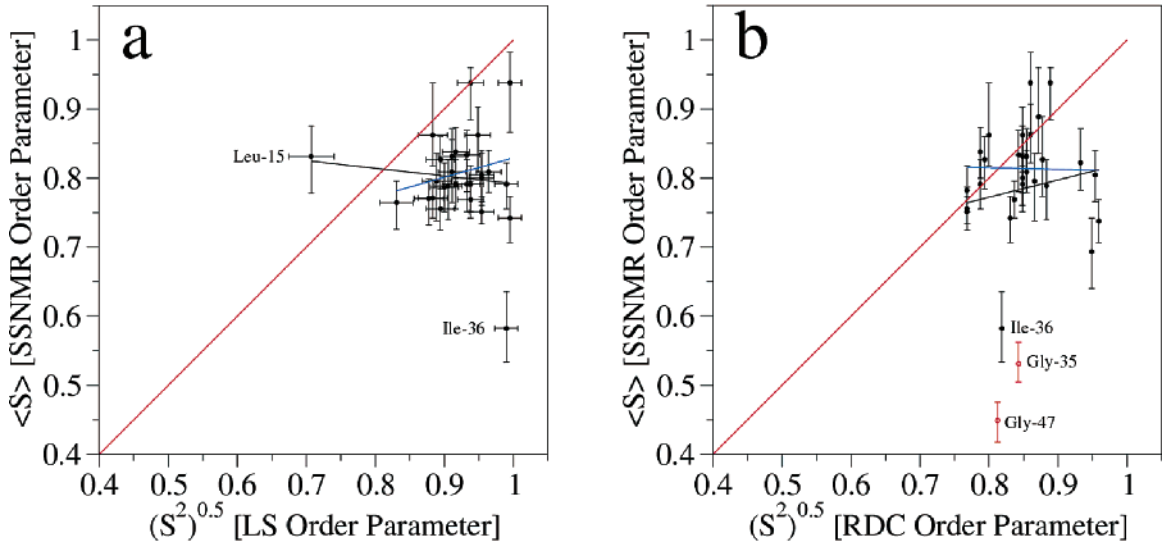

Figure 4. Comparison of liquid-phase NMR and solid-state NMR (SSNMR) ($^{13}C^1H_x$)α order parameters for ubiquitin. (a) The $^{13}C^1H$ solution NMR Lipari−Szabo (LS) generalized order parameters compared to the solid-state NMR order parameters. The blue linear regression line is $\langle S\rangle$ (SSNMR) = 0.548 + 0.281 $(S^2)^{0.5}$, (CC = 0.22) with the Leu-15 and Ile-36 outliers removed; the black linear regression with all points is $\langle S\rangle$ (SSNMR) = 0.903−0.111$(S^2)^{0.5}$, (CC = −0.10). The solution NMR data are measured at 30 °C at pH 5.7, and they are reproduced from Wand et al.[20] (b) The $^{15}N^1H$ RDC-based solution NMR order parameters compared to the solid-state NMR order parameters. The blue linear regression line shown is $\langle S\rangle$ (SSNMR) = 0.835−0.0244 $(S^2)^{0.5}$, (CC = −0.02) with the Gly-35, Ile-36, and Gly-47 outliers removed; the black linear regression with all points is $\langle S\rangle$ (SSNMR) = 0.572 + 0.250$(S^2)^{0.5}$, (CC = 0.12). The RDC-based data are measured at 35 °C at pH 6.5, and they are reproduced from Lakomek et al.[46] A 1:1 line is drawn in red to show that most SSNMR order parameters are lower than the solution NMR order parameters. The outliers are labeled according to residue number on the graph. The SSNMR order parameter is averaged on a picosecond to submicrosecond time scale. On the other hand, the solution Lipari−Szabo generalized order parameter is averaged on a subnanosecond time scale, and the RDC-based order parameter is averaged on a submicrosecond time scale. There is no direct correlation between the SSNMR and the Lipari−Szabo relaxation order parameters (weakly negative correlation), but there is a weak positive correlation between the SSNMR and RDC-based order parameters. Furthermore, the SSNMR order parameters are smaller than both the Lipari−Szabo and RDC-based order parameters.

bridge is maintained in the solution state.[41] Possible changes in the salt bridge structure in the MPD microcrystalline preparation at 17 °C could make Ile-36 more dynamic; residues Gly-35 and Ile-36 have order parameters around ∼0.55, and residue Glu-34 is missing from the data. In contrast, the outlier above the 1:1 line at (0.71, 0.83) is the Leu-15 ($^{13}C^1H$)α bond, which has a solid-state order parameter larger than that in solution.

By contrast, many of the RDC-based order parameters are closer to the 1:1 line. The measurement of RDC-order parameters in multiple aligned media produces order parameters that are thought to be averaged on a submicrosecond time scale.[42,43] Solution NMR studies have indicated the presence of motion on the microsecond time scale for residues Gln-40 and Ser-57[44] as well as residues Thr-7, Asp-20, Ile-23, Asn-25, Arg-54, Ser-65, and Val-70.[45,46] Clearly, the comparison of the RDC-based order parameters in this study confirms the additional motion that occurs on a time scale longer than a few nanoseconds—the tumbling time of ubiquitin in solution.

Correlations with Surface Exposure. Residues that are more solvent accessible may have a larger volume for local molecular motion, and therefore, a relationship between the solvent accessible surface area (SASA) and the amplitude of motion (i.e., the order parameter) might intuitively be expected. However, crystal packing interactions complicate the distinction of core and surface residues in considering local packing of microcrystalline samples.

We calculated the SASA with the GETAREA program,[47] which reports the ratio of area exposed of a residue to its random-coil value in a Gly-X-Gly tripeptide (averaged over 30 conformers).[48] Residues with a high surface area % to random-coil values are closer to the protein surface; residues with low area % to random-coil are buried in the protein core. It is thought that side chains of residues at the protein core may be more sterically strained as a result of tight packing,[49] and surface residues are solvent exposed, and the accessible volume for motion of the side chain is greater. For comparison, a detailed study on the structural effects of solution NMR $^{15}N^1H$ order parameters was conducted by Goodman et al.,[50] and it was found that solution relaxation order parameters do not correlate with the SASA.

A plot of the ($^{13}C^1H_x$)α and ($^{13}C^1H_x$)β order parameters against the surface exposure for each residue can be found in the Supporting Information. The linear regression correlation coefficients are low for all of the fits (much lower than |0.5|), demonstrating a low correlation in SASA to the ($^{13}C^1H_x$)α and ($^{13}C^1H_x$)β order parameters.

Experimental Bias in the Order Parameter Measurements. In principle, the reported heteronuclear dipolar coupling

(41) Cornilescu, G.; Marquardt, J. L.; Ottiger, M.; Bax, A. *J. Am. Chem. Soc.* **1998**, *120*, 6836−6837.
(42) Wang, M. F.; Bertmer, M.; Demco, D. E.; Blumich, B. *J. Phys. Chem. B* **2004**, *108*, 10911−10918.
(43) Schroder, L.; Schmitz, C.; Bachert, P. *J. Magn. Reson.* **2004**, *171*, 213−224.
(44) Tolman, J. R.; Al-Hashimi, H. M.; Kay, L. E.; Prestegard, J. H. *J. Am. Chem. Soc.* **2001**, *123*, 1416−1424.
(45) Peti, W.; Meiler, J.; Bruschweiler, R.; Griesinger, C. *J. Am. Chem. Soc.* **2002**, *124*, 5822−5833.
(46) Lakomek, N. A.; Carlomagno, T.; Becker, S.; Griesinger, C.; Meiler, J. *J. Biomol. NMR* **2006**, *34*, 101−115.
(47) Fraczkiewicz, R.; Braun, W. *J. Comput. Chem.* **1998**, *19*, 319−333.
(48) Oezguen, N. S., K.; Zhu, H.; Fraczkiewicz, R.; Braun, W. *Solvent Accessible Surface Areas, Atomic Solvation Energies, and Their Gradients for Macromolecules*, 2005. http://www.scsb.utmb.edu/cgi-bin/get_a_form.tcl.
(49) Gerstein, M.; Tsai, J.; Levitt, M. *J. Mol. Biol.* **1995**, *249*, 955−966.
(50) Goodman, J. L.; Pagel, M. D.; Stone, M. J. *J. Mol. Biol.* **2000**, *295*, 963−978.

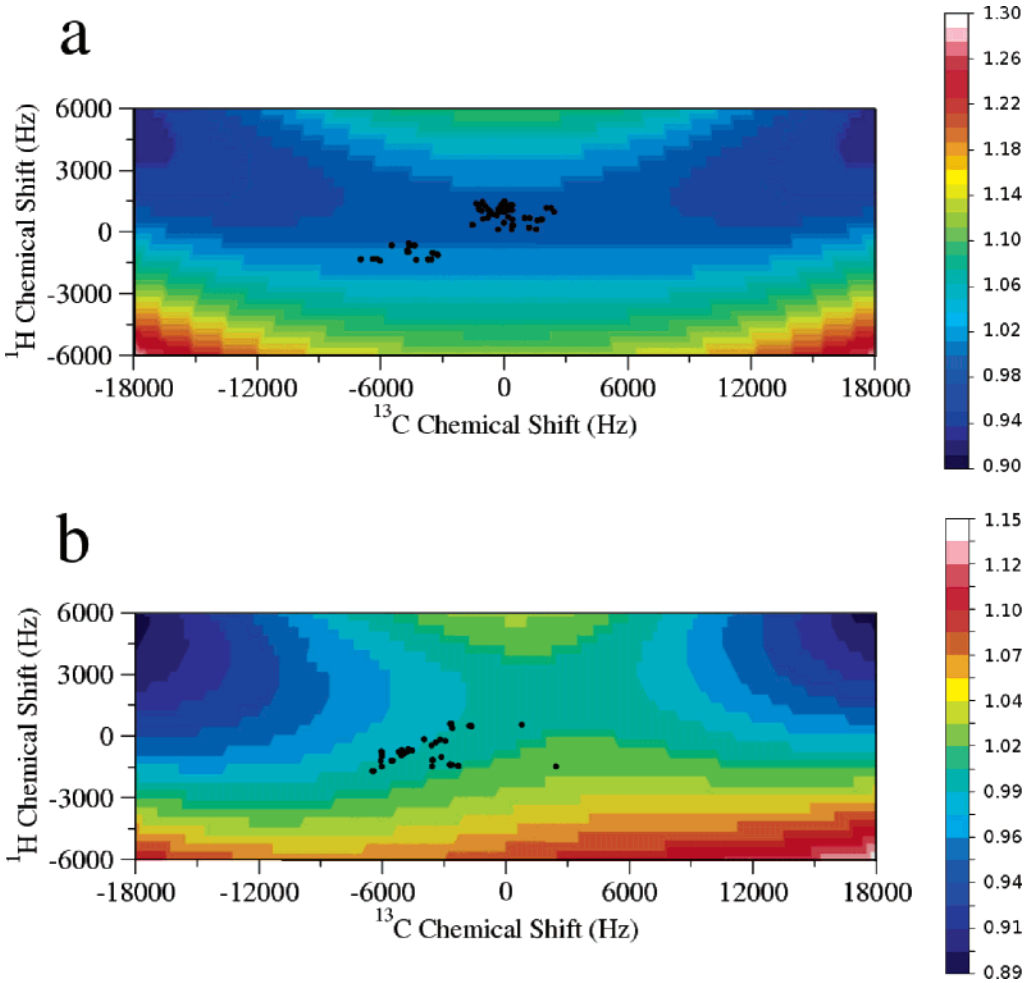

Figure 5. LGCP simulations showing the effect of the isotropic chemical shift on the $^{13}C^1H$ and $^{13}C^1H_2$ order parameters. The contour plot shows the relative scaling constant as a function of the ^1H and ^{13}C chemical-shift. The cross-peak chemical shifts are shown for the (a) $^{13}C^1H$ and (b) $^{13}C^1H_2$ spin systems. The black data points represent the experimental ^{13}C chemical shifts (in the t_2 dimension) and solution NMR ^1H chemical shift for all dipolar spectra measured.[51,52] For the 750 MHz spectrometer used in these experiments, the axes in units of ppm are ±8.0 ppm for the ^1H chemical shift and ±95.4 ppm for the ^{13}C chemical shift. Although large chemical shift offsets may produce differences in the line shape, the scaling constant was measured from the peak-to-peak splitting in the dipolar powder patterns. The on-resonance ($\omega_{1H,CS} = 0$ kHz, $\omega_{13C,CS} = 0$ kHz) simulation has an order parameter of 1.0.

could be different from the actual value due to absolute and/or relative scaling of the dipolar coupling constant (DCC). Absolute scaling denotes changes that affect all order parameters uniformly. Such an error could arise from an incorrect static limit $^{13}C^1H_x$ heteronuclear dipolar coupling constant or by improperly calibrating the LG fields. Relative scaling denotes differences in order parameters within the dataset that do not originate from differences in mobility.

In a study from our group,[33] the accuracy of LGCP for measuring $^{13}C^1H_x$ heteronuclear dipolar order parameters was investigated. For the static limit systems, which include alanine and glycine, the correct dipolar coupling constants were acquired within χ^2 fitting error. However, in the current experiments, absolute scaling errors could be more significant for a few reasons. The $^{13}C^1H_x$ heteronuclear scaling constant is directly related to the ω_{offset} and ω_{1H} fields. In these experiments, probe limitations reduced the proton fields to lower magnitudes (on the order of ~50 kHz), and the error in the scaling constant is greater as a result. Furthermore, calibration of these fields in a protein sample is more challenging because of the reduced signal-to-noise ratio. A realistic error of 2 kHz in both ω_{offset} and ω_{1H} fields produces an error estimate of 0.05 in the scaling constant for all sites.

Relative biases are more alarming because they artificially increase or reduce differences in mobility between sites, which can easily be misinterpreted as dynamic phenomena. The most evident form of relative bias arises from chemical shift differences between sites. For ^1H nuclei, the isotropic and anisotropic chemical shift Hamiltonians have spin tensors that are undifferentiated from the RF frequency offset Hamiltonian. The isotropic chemical shift is not suppressed from MAS, and it will contribute directly to the offset Hamiltonian. On the other hand, the zeroth order average of the time-dependent CSA is zero, and it should not contribute significantly for small CSA interactions.

To illustrate the effect of isotropic chemical shift on the relative scaling of the order parameter, LGCP simulations were conducted for the $^{13}C^1H$ and $^{13}C^1H_2$ spin systems. In Figure 5, a contour plot is shown for the scaling constant as a function of the ^1H and ^{13}C isotropic chemical shift for $^{13}C^1H$ and $^{13}C^1H_2$ spin systems. The on-resonance scaling constant is 1.0. Relative errors do not exceed 0.03 for the chemicals shifts measured in this study, and most are smaller than 0.02. From these simulations, relative errors do not exceed the χ^2 fitting errors in this study.

To further illustrate this effect, the $^{13}C^1H_x\alpha$ and $^{13}C^1H_x\beta$ order parameters do not have a correlation to the SSNMR ^{13}C chemical shift and solution NMR ^1H chemical shift[51,52]—a figure can be found in the Supporting Information. Although dynamics will introduce scatter in the data, a clear trend would be observable if the isotropic chemical shift was a dominant effect in the order parameter measurement.

From the simulations in Figure 5, we see that very large isotropic chemical shift differences have a noticeable effect on the order parameter. Measurements at much higher B_0 fields may become problematic for the relative errors in order parameters due to chemical shift differences. The $^1H/^{13}C$ chemical shifts from the 750 MHz NMR instrument in this study are dispersed over a small range compared to the experimental effective field, ω_{eff}, and the largest relative error between order parameters is around ± 0.02 for most sites. Ideally, measurements at a different ω_1 field would be desirable, but this experiment was not conducted because the highest achievable field on the 750 MHz NMR instrument was at the lower limit for homonuclear decoupling. Figure 5 also shows that $^{13}C^1H$ spin systems are more sensitive to ^1H chemical shift offsets and $^{13}C^1H_2$ spin systems are more sensitive to ^{13}C chemical shift offsets.

The is no correlation between the order parameter and the ^{13}C or ^1H chemical shift. A linear regression analysis of the order parameters as a function of their ^1H and ^{13}C chemical shifts show that the chemical shift bias on the order parameter is around 0.04. There is a small relative error due to the isotropic chemical-shift that is comparable in magnitude to the χ^2 fitting error.

In theory, the order parameter measurement can be biased by factors that change the scaling constant homogeneously for all sites (absolute scaling) or by factors that change the scaling constant for different sites (relative scaling). The dominant factor in absolute scaling is the miscalibration of nutation and/or offset fields. These factors depend on the instrumentation and the experimentalist. On the other hand, relative errors originate from differences in site-to-site Hamiltonians, structure, and dynamics. The ^{13}C and ^1H chemical shifts directly affect the scaling constant, and this effect can be quite significant for large chemical shift differences. However, these sources of bias are estimated to be of the same order as the dipolar fit error (0−0.04 order parameter units). Furthermore, differences in $^{13}C^1H_x$ bond lengths could change the order parameters, and a measurement at a very cold temperature, such that all order parameters are 1.0, would be useful in ascertaining this issue.

Conclusion

In summary, the backbone and side-chain order parameters of microcrystalline ubiquitin provide evidence for a highly dynamic protein molecule in the crystalline state. On the fast-limit time scale, large-amplitude reorientations occur in the backbone $(^{13}C^1H)\alpha/(^{13}C^1H_2)\alpha$ and the side-chain $(^{13}C^1H)\beta/(^{13}C^1H_2)\beta$ sites throughout the molecule. It was found that more highly substituted sites have more inhibited motion and that backbone and side-chain order parameters are similar for residues of the same amino acid type.

In the analysis of measurement bias, it was found that the relative and absolute error in these measurements does not exceed the error of the dipolar fit. The measurement of solid-state NMR order parameters complements structural studies of protein biophysics and broadens our understanding of catalysis and function in solid-state biomolecular systems.

Acknowledgment. We acknowledge funding support from the NIH (NIH R01GM066388) and the New York Structural Biology Center (NYSBC). We also thank Arthur G. Palmer (Columbia University) for helpful comments on the manuscript. Support for the NYSBC has been provided by NIH/NIGMS through Grant P41 GM66354.

Supporting Information Available: Plots of the $(^{13}C^1H_x)\alpha$ and $(^{13}C^1H_x)\beta$ order parameters against the surface exposure for each residue, pulse sequence diagram. This material is available free of charge via the Internet at http://pubs.acs.org.

JA062443U

(51) Distefano, D. L.; Wand, A. J. *Biochemistry* **1987**, *26*, 7272−7281.
(52) Weber, P.; Brown, S.; Mueller, L. *Biochemistry* **1987**, *26*, 7282−7290.
(53) Laskowski, R. A.; Chistyakov, V. V.; Thornton, J. M. *Nucleic Acids Res.* **2005**, *33*, D266−D268.
(54) Laskowski, R. A. *Nucleic Acids Res.* **2001**, *29*, 221−222.